EPMA Journal (2019) 10:249–259
https://doi.org/10.1007/s13167-019-00171-4

RESEARCH

The predictive potential of altered spontaneous brain activity patterns in diabetic retinopathy and nephropathy

Yu Wang[1] · Yi Shao[2] · Wen-Qing Shi[2] · Lei Jiang[1] · Xiao-yu Wang[1] · Pei-Wen Zhu[2] · Qing Yuan[2] · Ge Gao[3] · Jin-Lei Lv[1] · Gong-Xian Wang[4]

Received: 29 January 2019 / Accepted: 12 May 2019 / Published online: 5 July 2019

Abstract

Objective The amplitude of low-frequency fluctuation (ALFF) fMRI technique was used to study the changes of spontaneous brain activity in patients with diabetic retinopathy and nephropathy (DRN), and to explore the application of ALFF technique in the potential prediction and the targeted prevention of diabetic microangiopathy.

Methods Nineteen patients with diabetic retinopathy and nephropathy and 19 healthy controls (HCs) were matched for age and gender. Spontaneous cerebral activity variations were investigated using the ALFF technique. The average ALFF values of the DRN patients and the HCs were classified utilizing receiver operating characteristic (ROC) curves.

Results In contrast to the results in the HCs, the patients with DRN had significantly higher ALFF values in the cerebellum (bilaterally in the posterior and anterior lobes) and the left inferior temporal gyrus, but the ALFF values of the bilateral medial frontal gyrus, right superior temporal gyrus, right middle frontal gyrus, left middle/inferior frontal gyrus, bilateral precuneus, and left inferior parietal lobule were lower. ROC curve analysis of each brain region showed the accuracy of AUC was excellent. However, the mean ALFF values in the different regions did not correlate with clinical performance. The subjects showed abnormal neuronal synchronization in many areas of the brain, which is consistent with cognitive and visual functional deficits.

Conclusion Abnormal spontaneous activity was detected in many areas of the brain, which may provide useful information for understanding the pathology of DRN. Abnormal ALFF values of these brain regions may be of predictive value in the development of early DRN and be a targeted intervention indicator for individualized treatment of diabetic microvascular diseases.

Keywords Predictive preventive personalized medicine · ALFF · fMRI · Diabetic retinopathy · Diabetic nephropathy · Diabetic microvascular diseases · Resting state · Spontaneous brain activity

Introduction

Diabetic retinopathy (DR) is a common microvascular complication of diabetes [1] and is a leading cause of visual loss. The number of DR patients is increasing globally, which reflects the increasing lifespan of diabetic patients [2]. The earliest clinical signs of diabetic retinopathy are microaneurysms that are seen as small areas of abnormal retinal capillaries and punctate retinal hemorrhages during funduscopy [3]. The emergence of new blood vessels in DR indicates formation of proliferative diabetic retinopathy (PDR), which is characterized by retinal angiogenesis and fibrosis. The development of PDR is related to various growth factors [4], including VEGF, Ang2, NP1, and RSR. Compared with non-proliferative diabetic retinopathy (NPDR), PDR has more impact on vision and can lead to vitreous hemorrhage, retinal detachment, and neovascularization, with formation of new

Yu Wang and Yi Shao contributed equally to this work.

✉ Ge Gao
gaogebj@sina.com

✉ Jin-Lei Lv
lvjinlei97@163.com

[1] Department of Nephrology, The First Affiliated Hospital of Nanchang University, No 17, YongWaiZheng Street, Nanchang 330006, Jiangxi, People's Republic of China

[2] Department of Ophthalmology, The First Affiliated Hospital of Nanchang University, Nanchang 330006, Jiangxi, China

[3] Department of General Surgery, The First Affiliated Hospital of Nanchang University, No 17, YongWaiZheng Street, Nanchang 330006, Jiangxi, People's Republic of China

[4] Department of Urinary Surgery, The First Affiliated Hospital of Nanchang University, Nanchang 330006, Jiangxi, China

blood vessels that can block the outflow of aqueous fluid, resulting in increased intraocular pressure and neovascular glaucoma, severe pain, and even complete blindness [3].

Diabetic nephropathy (DN), also called diabetic kidney disease, is caused by a chronic loss of kidney function in diabetic patients [5]. Epidemiological studies show that the incidence of diabetic nephropathy in both the USA and India is more than 30% [6, 7]. It is common in diabetic patients with a disease duration over 10 years [8]. Microalbuminuria has long been a diagnostic marker for early diabetic nephropathy. However, studies have shown that diabetic microalbuminuria patients are only 30 to 35% likely to develop albuminuria within 10 years [9]. Diabetic retinopathy is now recognized as a more sensitive indicator of diabetic nephropathy, according to the Kidney Disease Outcomes Quality Initiative (KDOQI) clinical practice guidelines [10]. In a study in diabetic rats, Cherian et al. [11] found that the thickening of retinal capillary and glomerular capillary basement membranes were both associated with fibronectin expression in the glomerular capillaries. Kramer et al. [12] reported that diabetic nephropathies and retinopathies both involve similar microvascular lesions. The blood vessels of the brain and retina have similar anatomical, physiological, and metabolic characteristics, and many of the neuroimaging markers of diabetic brain abnormalities are associated with microvascular disease [13]. Patients with DR are reported to be at increased risk of developing kidney and cardiovascular disease [14]. Often, the first symptom of early diabetic nephropathy is nocturnal polyuria [9], and other symptoms include fatigue, headache, general signs of illness, nausea, vomiting, frequent daytime urination, loss of appetite, altered mental states, and edema of the lower extremities [15]. At present, there are few studies of changes of brain function with DRN. We hypothesized that the presence of DRN may indicate that there is parallel brain parenchymal damage caused by microvascular lesions in these patients and that abnormal amplitude of low-frequency fluctuation (ALFF) values recorded from these brains may be new predictors of early DRN. We hope that this technique could contribute to the early diagnosis of diabetic nephropathy.

Because diabetic nephropathy is a complex metabolic disorder, once it develops into end-stage renal disease, it is often more difficult to treat than other kidney diseases. Functional magnetic resonance imaging (fMRI) can help detect changes in the human brain [16, 17] and enhance our knowledge of central nervous system pathology. It thus is of great value to elucidate the pathophysiology and mechanisms of disease [18]. Resting-state functional magnetic resonance imaging (rs-fMRI) has been extensively used to study brain function while the patient is at rest and not performing specific tasks [19]. ALFF values are one resting-state fMRI method to assess the activity of the idle brain [20]. Studies have shown that ALFF values perform well with respect to test–retest reliability [18, 21]. We had successfully used ALFF values in previous studies to assess the neurological status of patients with eye diseases such as optic neuritis [22], glaucoma [23], strabismus [24], and amblyopia [25] (Fig. 1).

Materials and methods

Subjects

The study enrolled 19 patients with DRN from the First Affiliated Hospital of Nanchang University between May 2017 and July 2018. The inclusion standards for the study were as follows: (1) diagnosed diabetes mellitus, (2) diagnosis of end-stage diabetic nephropathy: stage 4 or 5, (3) no evidence of brain parenchymal disease on a cranial MRI, and (4) no other ocular disease in either eye (including retinal degeneration, glaucoma, cataracts, amblyopia, optic neuritis, strabismus). Since we selected hospitalized patients in the Department of Nephrology, whose renal function had progressed to a poor state. So, the inclusion criteria were in stage 4 or 5 of diabetic nephropathy. The exclusion criteria were as follows: (1) long-term medical treatment of blindness, (2) a history of surgery in both eyes, (3) bilateral late blindness or congenital blindness, and (4) mental illness (such as mania, depression, or schizophrenia) or brain parenchymal injury. Nineteen patients with DRN, and 19 appropriate controls, were recruited and matched according to age, educational status, and sex. All of the participants conformed to the subsequent criteria: (1) cranial MRIs that revealed no apparent deformities in the brain parenchyma, (2) no drug or alcohol addiction, (3) no known psychiatric diseases, cerebral infarctions, or cardiovascular diseases, (4) capable of completing MRI examinations, and (5) no known genetic diseases in their family history.

This study conformed to the precepts of the Declaration of Helsinki and was performed pursuant to formal approval by the Medical Ethics Committee of the First Affiliated Hospital of Nanchang University. All volunteer subjects of the study signed informed consent forms after having the objectives, content, and latent risks of the research protocol explained to them, and having any questions answered by an investigator.

Methods

Diagnostic criteria

The new DR international classification standard developed by the congress of the International Council of Ophthalmology in Sydney in 2002 as follows: (1) after early mydriasis, funduscopy showed that the posterior pole of the retina had diffuse microaneurysms and small spots or patches

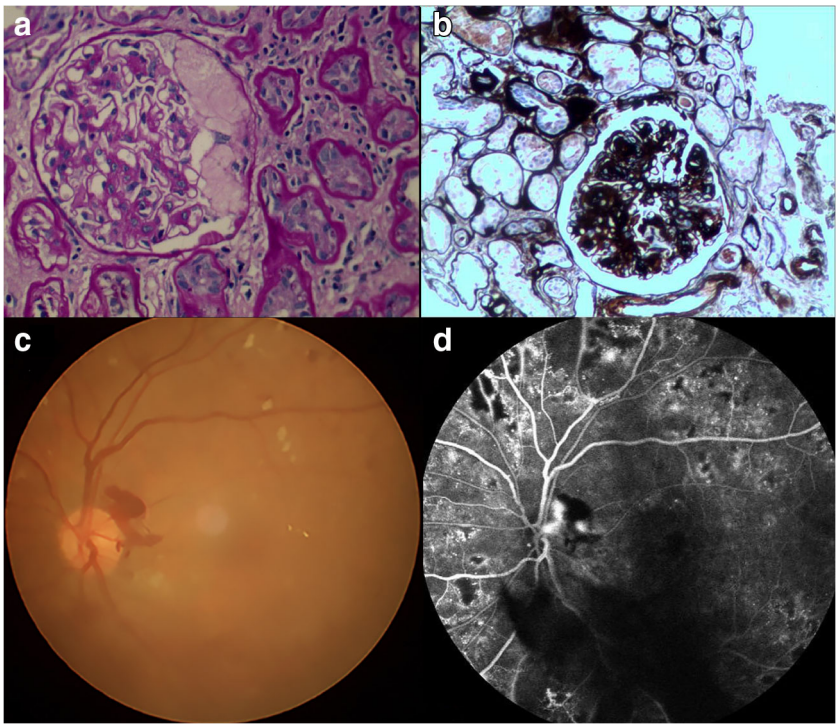

Fig. 1 Example of diabetic retinopathy and nephropathy (DRN) seen on renal biopsy and retinal fundus. Hematoxylin-eosin staining (**a**) and cyclic acid-silver-methylamine staining (**b**) of renal tissue showed severe dilation of mesangial matrix and tuberous sclerosis of glomerulus. Funduscopy (**c**) showed that the retina had diffuse microaneurysms and patches of hemorrhage. The fluorescein fundus angiography (**d**) showed a significant increase in the number of retinal microangiomas

of hemorrhage. Some patients could see white or yellowish white exudation, and the visual acuity of the patients was decreased; (2) ocular angiography revealed retinal lesions in the fundus; (3) fluorescein angiography of the fundus showed that the number of microangiomas was obviously increased, to a larger extent than that revealed by fundic microscopy alone, and the capillaries around the retina were dilated, with increased permeability and abnormal findings [26]. Documentation of any of the above findings in this part of the study led to a diagnosis of diabetic retinopathy.

Five stages of diabetic nephropathy were recognized according to the following diagnostic criteria: phase I, with a normal glomerular filtration rate (GFR > 90 ml/min/1.73 m^2) and no clinical symptoms. Phase II, showing normal urinary albumin or microalbuminuria with an ACR < 30 μg/gCr, and a GFR of 60 to 89 ml/min/1.73 m^2. Phase III, showing early diabetic nephropathy with an ACR between 30 and 300 μg/gCr and a GFR of 30 to 59 ml/min/1.73 m^2. Phase IV, after the advent of diabetic nephropathy and massive proteinuria, with ACR > 300 μg/gCr and > 0.5 g urinary protein/24 h, with a GFR 15 to 29 ml/min/1.73 m^2. Phase V, or advanced diabetic nephropathy, with a GFR < 15 ml/min/1.73 m^2 and frank uremia. Staging of nephropathy was carried out according to this document [10].

MRI parameters

A Trio 3-Tesla MR scanner (Siemens, Munich, Germany) was used to perform the MRI. All the subjects were asked to keep their eyes closed while awake in the scanner and to maintain normal breathing patterns until the study was completed [23]. A 3D spoiled gradient recalled-echo pulse sequence was applied to acquire the functional data, with parameters as follows: for 176 structural image scans, we used an acquisition matrix = 256 × 256, field of view = 250 × 250 mm, echo time = 2.26 ms, repetition time = 1900 ms, thickness = 1.0 mm, gap = 0.5 mm, and a flip angle = 9°. For 240 functional image scans, we utilized an acquisition matrix = 64 × 64, field of view = 220 × 220 mm, thickness = 4.0 mm, gap = 1.2 mm, repetition time = 2000 ms, echo time = 30 ms, flip angle = 90°, and 29 axials. Each of the MRI examinations lasted for about 15 min.

Data analysis for the fMRI scans

Our previous reports described the method of functional data analysis. We first applied MRIcro software to identify and delete incomplete data. During the magnetization equilibration phase, the first 15 time points were discarded. Data Processing Assistant for the advanced edition of Resting-State fMRI (DPARSFA 4.0, http://rfmri.org/DPARSF) software was used for head motion correction, spatial normalization, slice timing, the form conversion of digital imaging communications in medicine (DICM), and full-width smoothing with a Gaussian kernel of 6 × 6 × 6 mm^3 at half-maximum, based on the rs-fMRI data analysis toolkit (REST, http://www.restfmri.net) and Statistical Parametric Mapping software (SPM, http://www.fil.ion.ucl.ac.uk/spm). Subjects were

excluded if they had 1.5 angular motion or if the maximum offset of the x, y, or z directions exceeded 1. 5 mm during the fMRI examination. Head motion artifacts were removed using the technique of Friston et al. since higher-order models were recently reported to be more effective [27, 28]. We also utilized linear regression to remove false covariates and their temporal derivatives from a variety of other sources, including signals from regions of interest (ROI) to the ventricle and the white matter-centered region [29]. In the current data, the global signal did not shrink as it did in our previous studies [18, 30, 31]. This may relate to the elimination of global signals during the resting-state data preprocessing [32, 33]. The fMRI images were unified to the spatial standards of the Montreal Neurological Institute & Hospital using an echo plane imaging template after the head motion correction, and the images were resampled with a resolution of 3 mm × 3 mm × 3 mm at the same time. After pretreatment, the time series of each voxel decreased linearly to reduce the low-frequency drift, heart noise, and physiological high frequency respiration, along with time series linear detrending. In order to reduce the impact of variability between participants, we divided the ALFF of each voxel by the global average ALFF value of each subject.

Statistical analysis

The clinical variables and demographics of the DRN and HC groups were compared with SPSS software, version 20.0 (IBM Corp., Armonk, NY, USA) via *t* tests for independent samples. Differences were considered to be statistically significant when $p < 0.05$. Functional data were compared using the two-sample *t* test in REST software. Using Gaussian random field theory, the statistical threshold of voxel level for multiple comprehensive comparisons was again set at a level of $p < 0.05$. And Alphasim corrected at a cluster size > 40 voxels and a level of $p < 0.01$.

The mean ALFF values in regions of the cerebrum were significantly different between the subjects and HCs, as classified by receiver operating characteristic (ROC) curves.

Results

Demographics and behavioral results

There were no statistically significant differences between these two groups ($p > 0.05$) in weight ($p = 0.117$) or age ($p = 0.593$) as shown in Table 1. And the mean ± standard deviation of the DRN duration was 12.32 ± 5.26 days (Table 1).

ALFF differences

In contrast to the findings in the HCs, the ALFF values of the patients with DRN were significantly lower in the bilateral medial frontal gyrus, right superior temporal gyrus, right middle frontal gyrus, left middle/inferior frontal gyrus, bilateral precuneus, and left inferior parietal lobules, but higher ALFF values were found bilaterally in the cerebellar posterior/anterior lobes and the left inferior temporal gyrus (see Figs. 2 and 3 and Table 2).

ROC curve

Receiver-operator curves (ROC) were used to analyze the mean ALFF values of the different brain areas. The area under the ROC curve (AUC) showed the diagnosis rate. The AUCs of the ALFF values of the different brain regions were as follows: bilateral cerebellar posterior/anterior lobes (0.994, $p < 0.001$), left inferior temporal gyrus (0.938, $p < 0.001$) (Fig. 4a), bilateral medial frontal gyrus (0.964, $p < 0.001$), right superior temporal gyrus (0.895, $p < 0.001$), right middle frontal gyrus (0.956, $p < 0.001$), left middle/inferior frontal gyrus (0.953, $p < 0.001$), bilateral precuneus (0.873, $p < 0.001$), right middle frontal gyrus (0.936, $p < 0.001$), and left inferior parietal lobule (0.917, $p < 0.001$) (Fig. 4b).

Table 1 Demographic data for DRN and HCs

	DRN	HCs	*t* value	*p* value
Male/female	8/11	8/11	N/A	> 0.99
Age (years)	53.12 ± 8.02	54.22 ± 9.02	0.512	0.593
Weight (kg)	60.18 ± 9.91	59.38 ± 9.03	1.312	0.117
Scr (umol/l)	272.22 ± 111.93	N/A	N/A	N/A
ACR (mg/g)	2131.42 ± 1326.37	N/A	N/A	N/A
Diabetes duration (year)	12.32 ± 5.26	N/A	N/A	N/A

DRN, diabetic retinopathy with nephropathy; *HCs*, healthy controls; *Scr*, serum creatinine; *ACR*, urine albumin/creatinine ratio; *N*/A, not applicable

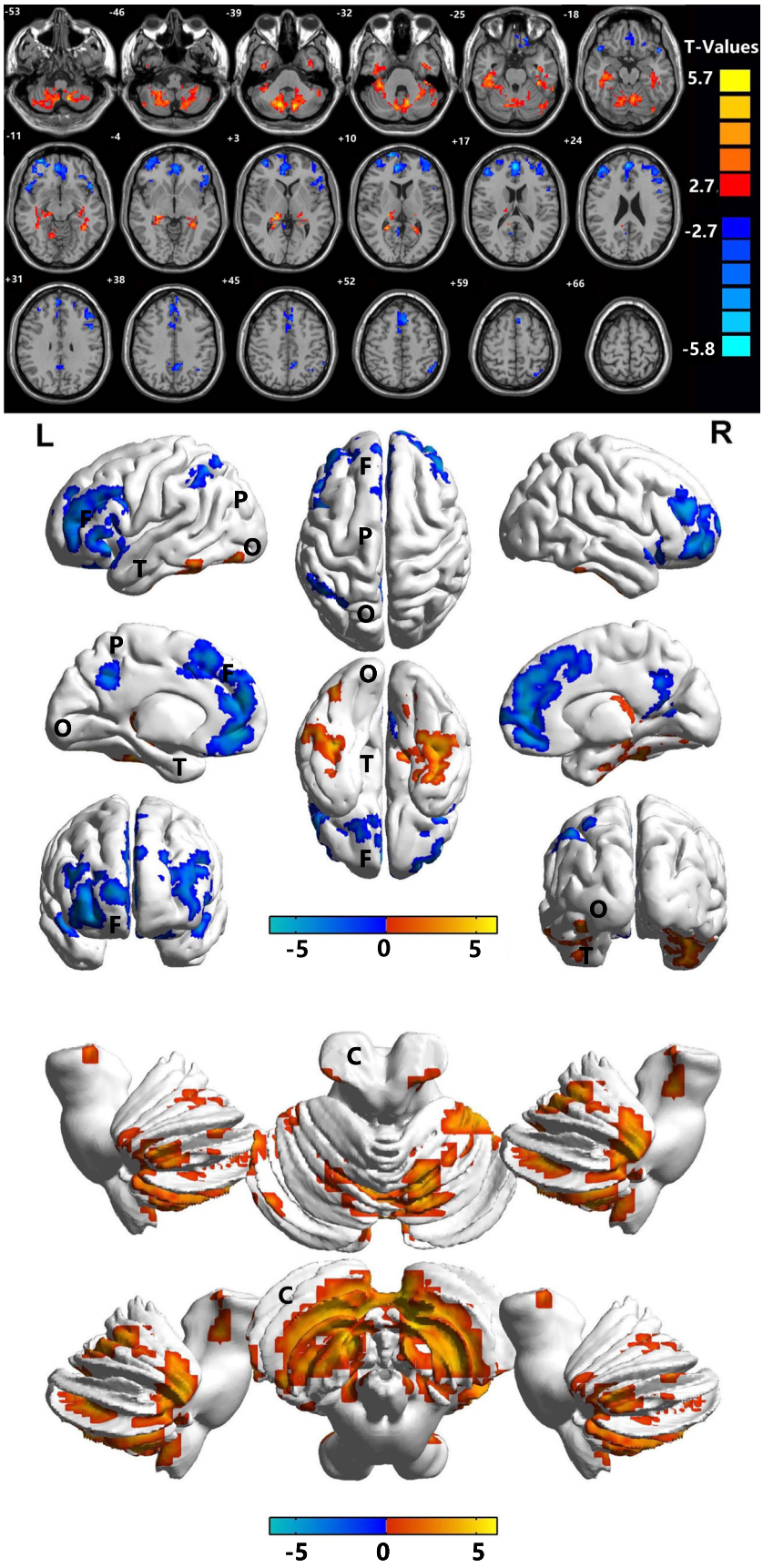

Fig. 2 Marked differences in spontaneous brain activity in the DRN group compared with HCs. Notes: The different brain regions were observed in the bilateral cerebellum posterior/anterior lobe, left inferior temporal gyrus, bilateral medial frontal gyrus, right superior temporal gyrus, right middle frontal gyrus, left middle/inferior frontal gyrus, bilateral precuneus, and left inferior parietal lobule in the DRN group. The red areas denote higher ALFF brain regions, and the blue areas denote lower ALFF brain regions. ALFF, amplitude of low-frequency fluctuation; HCs, healthy controls; L, left; R, right; B, bilateral; T, temporal lobe; F, frontal lobe; O, occipital lobe; C, cerebellum; P, parietal lobe

Discussion

The prevalence of diabetes is rapidly increasing worldwide, especially in Asian countries, and the epidemiology of this disease has significant public health implications based on its major long-term vascular complications. These actualities urge physicians to formulate and implement individualized medicine strategies for diabetes. It has led to a series of worldwide studies on the pathogenesis of diabetic complications, with the ultimate goal of targeted prevention of various diabetic complications and reduction of mortality. Tomino et al. [34] found that despite strict control of blood glucose and/or blood pressure, about 30–40% of patients with type 2 diabetes develop DN. Microvessels refer to capillaries and microvascular networks that form the vascular linkages with lumen diameters of less than 100 μm that carry the circulation between the terminal arteries and the smallest veins. Microvascular disease is a specific complication of diabetes, with typical changes being microcirculatory disorders and microvascular basement membrane thickening [35]. Microvascular disease can affect tissues and organs throughout the body, but mainly are diagnosed in the retina [36], kidney [37], and heart [38], as well as with neuropathies [39]. This pathology is commonly implicated in diabetic nephropathy and retinopathy. Previous research studies have found that patients with PDR often have diabetic nephropathy as well [39].

To our knowledge, this is the first study to investigate the correlation between DRN and interhemispheric functional changes using the ALFF method. In contrast to the results in the HCs, the DRN patients exhibited remarkably lower ALFF values in the medial frontal gyrus bilaterally, in the right superior temporal gyrus, the right middle frontal gyrus, the left middle/inferior frontal gyrus, the bilateral precuneus and the left inferior parietal lobule. But higher ALFF values occurred in the posterior/anterior lobes of the cerebellum bilaterally and in the left inferior temporal gyrus (Fig. 5). The ALFF method has been successfully applied in ophthalmological diseases and is predicted to have huge prospects for clinical development [25, 40–43].

The medial frontal lobe, located anterior to the paraspinal central lobule and passing forward across the cingulate gyrus, may also be regarded as the medial side of the superior frontal gyrus. It is considered to provide executive functions and processes related to decision-making [44]. In the medial frontal gyrus, there is an area called the frontal eye field (FEF), which controls spontaneous eye movements [45]. The medial frontal cortex is part of the default model network (DMN) [46] that has been associated with a variety of mental disorders, including depression [47]. The DMN is activated during rest and disabled during goal-oriented tasks. Many brain regions are involved in the DMN, including the inferior parietal cortex, middle frontal gyrus, superior frontal gyrus, and the precuneus [48, 49]. There is growing evidence that the brain regions of DMN play an important role in depression and anxiety [50]. Depression is common in patients with diabetes, especially in those with microvascular complications such as nephropathy and retinopathy [51]. Themeli et al. [52] found that 83% of their patients with diabetic nephropathy had depressive symptoms. The precuneus is in the parietal lobe and plays a key role in the coordination of movement, visuospatial imagery, and working memory [53]. Goffaux et al. found that in healthy adults, the precuneus was associated with pain sensitivity,

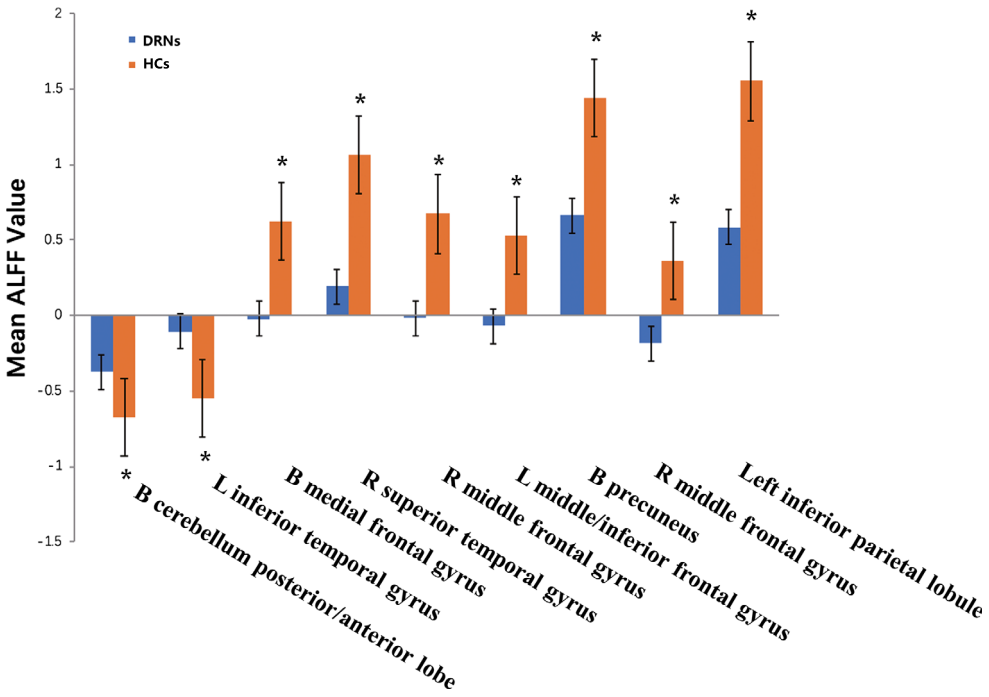

Fig. 3 Means of altered spontaneous brain activity between the DRN group and HCs group (each $n = 19$). Notes: Compared with HCs, asterisk means the statistical significance $p < 0.05$. HCs, healthy controls; ALFF, amplitude of low-frequency fluctuation; L, left; R, right; B, bilateral

Table 2 Brain areas with significantly different ALFF values between groups

Condition	Side	Brain regions	MNI coordinates			BA	Peak voxels	*t* value
			X	*Y*	*Z*			
DRNs>HCs								
1	B	Cerebellum posterior/anterior lobe	−9	−72	−39	/	1963	6.0348
2	L	Inferior temporal gyrus	−36	−36	−27	20	476	6.1407
DRNs<HCs								
1	B	Medial frontal gyrus	0	51	18	10	903	−6.2601
2	R	Superior temporal gyrus	48	21	−18	38	77	−4.925
3	R	Middle frontal gyrus	30	60	−9	11	285	−6.4547
4	L	Middle/inferior frontal gyrus	−48	18	−15	10	617	−5.6439
5	B	Precuneus	6	−57	12		119	−4.3607
6	R	Middle frontal gyrus	48	45	21	10	143	−5.2267
7	L	Inferior parietal lobule	−48	−57	54	40	64	−5.4047

*$p < 0.05$; #$p < 0.001$; independent *t* test, *p* values between DRNs and HCs

ALFF, amplitude of low-frequency fluctuation; *BA*, Brodmann area; *HCs*, healthy controls; *DRN*, diabetic retinopathy with nephropathy; *MNI*, Montreal Neurological Institute; *L*, left; *R*, right; *B*, bilateral

and an interfering DMN has been found in various pain-related diseases such as headache, dysmenorrhea, and chronic low back pain [54–56]. In support of these findings, the present study showed that lower ALFF values occurred bilaterally in the medial frontal gyrus, and in the right middle frontal gyrus, the left inferior parietal lobule, and bilaterally in the precuneus, while the higher ALFF values in the left inferior temporal gyrus may reflect compensation by the DMN in order to maintain the stability of the neural network.

The superior temporal gyrus is located on the temporal lobe between the lateral sulcus and the superior temporal sulcus. In

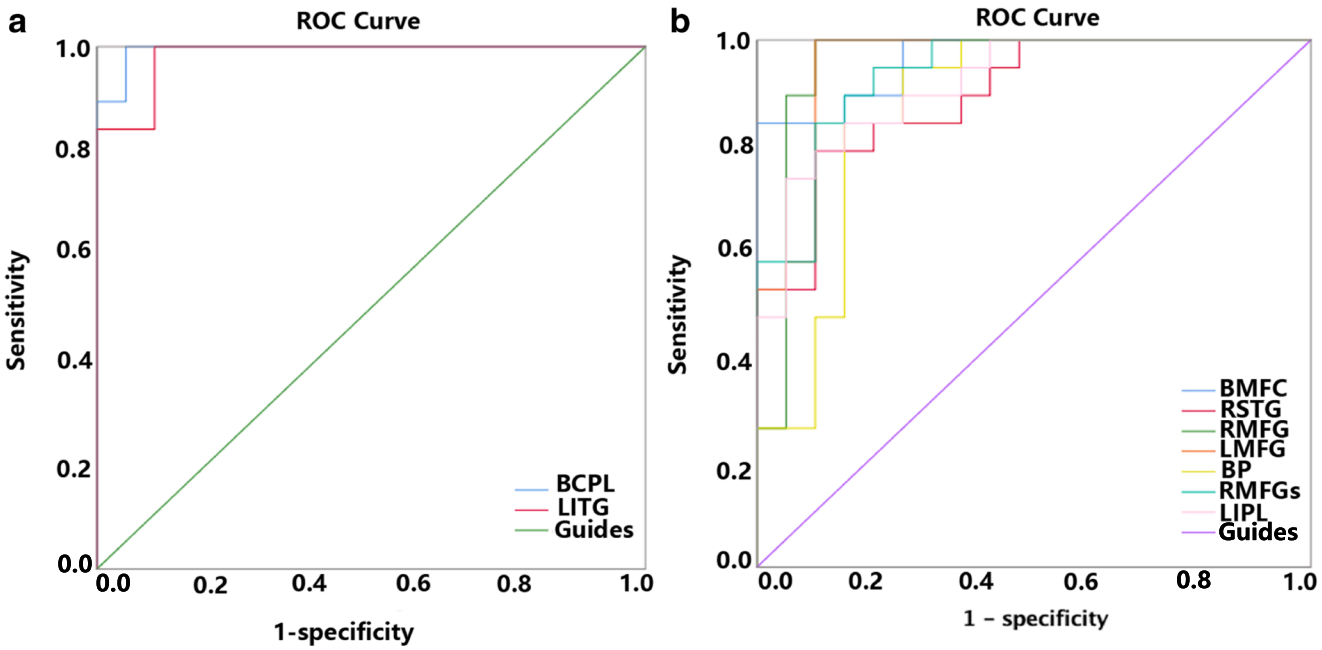

Fig. 4 ROC curve analysis of the mean ALFF values for altered brain regions. **a** The area under the ROC curve were 0.994 ($p < 0.001$; 95% CI 0.980–1.000) for BCPL, LITG 0.938 ($p < 0.001$; 95% CI 0.953–1.000) [UDs>HCs]. **b** The area under the ROC curve were 0.964 ($p < 0.001$; 95% CI 0.914–1.000) for BMFG, RSTG 0.895 ($p < 0.001$; 95% CI 0.797–0.992), RMFG 0.956 ($p < 0.001$; 95% CI 0.879–1.000), LMFG 0.953 ($p < 0.001$; 95% CI 0.885–1.000), BP 0.873 ($p < 0.001$; 95% CI 0.753–0.992), RMFGs 0.936 ($p < 0.001$; 95% CI 0.863–1.000), LIPL 0.917 ($p < 0.001$; 95% CI 0.832–1.000) [UDs<HCs]. ALFF, amplitude of low-frequency fluctuation; ROC, receiver operating characteristic; BCPL, bilateral cerebellum posterior/anterior lobe; LITG, left inferior temporal gyrus; BMFG, bilateral medial frontal gyrus; RSTG, right superior temporal gyrus; RMFG, right middle frontal gyrus; LMFG, left middle/inferior frontal gyrus; BP, bilateral precuneus; RMFGs, right middle frontal gyrus; LIPL, left inferior parietal lobule

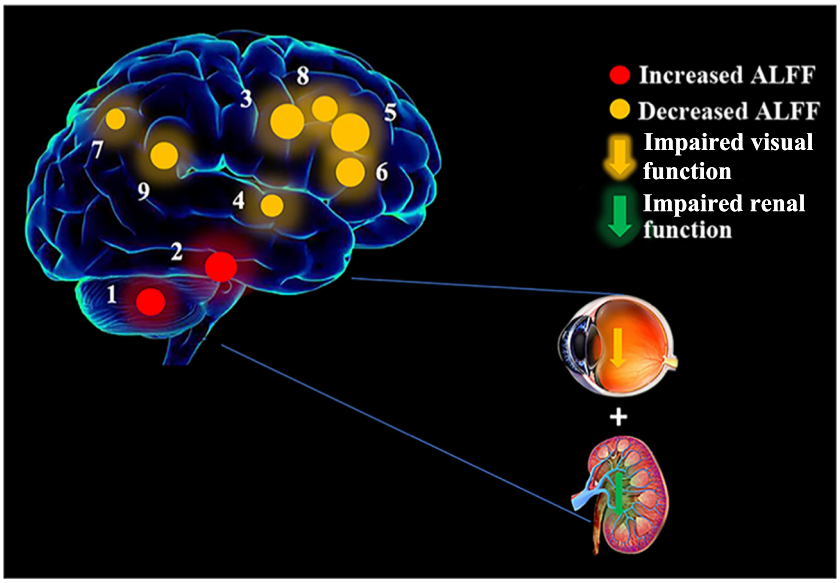

Fig. 5 The ALFF results of brain activity in the DRN group. Compared with the HCs, the ALFF of the following regions were increased to various extents: 1-bilateral cerebellum posterior/anterior lobe ($t = 6.0348$), 2-left inferior temporal gyrus ($t = 6.1407$), and decreased ALFF values in the 3-bilateral medial frontal gyrus ($t = -6.2601$), 4-right superior temporal gyrus ($t = -4.925$), 5-right middle frontal gyrus ($t = -6.4547$), 6-left middle/inferior frontal gyrus ($t = -5.6439$), 7-bilateral precuneus ($t = -4.3607$), 8-right middle frontal gyrus ($t = -5.2267$), and 9-left inferior parietal lobule ($t = -5.4047$). The sizes of the spots denote the degree of quantitative changes. HCs, healthy controls; ALFF, amplitude of low-frequency fluctuation; DRN, diabetic retinopathy and nephropathy

previous studies, dysfunction of the superior temporal gyrus has been associated with ocular diseases. Werring et al. [57] reported abnormal activation of the lateral temporal area in patients with optic neuritis. Wang et al. [58] found that patients with diabetic retinopathy had lower ALFF values than HCs in the superior temporal gyrus. Zhen et al. [59] reported that patients with strabismus amblyopia showed abnormal ALFF values as well. In our study, patients with DRN had decreased ALFF values in the superior temporal gyrus. Synthesizing the information above, we can speculate that decreased ALFF values in the superior temporal gyrus reflect the degree of intraocular inflammation and visual impairment in patients with DRN.

The cerebellum is involved in physical balance, motor coordination, and the execution of eye movements [60]. With the development and application of neuroimaging techniques in recent years, we have a further understanding of the role of the cerebellum in emotional processing. Timmann et al. [61] reported that visual impairment can cause a range of social and emotional problems. Morenorius et al. [62] reported a positron emission tomography (PET) study that showed abnormal signals in the cerebellum of patients with social anxiety, characterized by increased cerebellar blood flow, suggesting that the cerebellum is associated with anxiety. This is in line with our findings. The patients were generally nervous when fMRI scan was performed. In addition, Ikeda et al. [63] found that bleeding in patients with renal failure caused by diabetic nephropathy often involved the cerebellum. Generally speaking, in diabetics, both nephropathy and retinopathy represent microvascular complications. In our study, we found that the higher ALFF values occurred bilaterally in the posterior and anterior lobes of the cerebellum. Therefore, we speculated that diabetic retinopathy and diabetic nephropathy are both likely to lead to dysfunction of the cerebellum (Table 3). However, our experiment also has some limitations. First, all the DNR patients we selected were hospitalized, which were in advanced stage of diabetic nephropathy (stage 4 or 5). In the future, we will consider selecting patients with early diabetes and diabetic nephropathy from outpatient clinics and studying their brain changes. For the early diagnosis of diabetes, we will consider using some new tools for early diagnosis of diabetes, such as multihistology in liquid biopsy which will help us to study diabetic microangiopathy at multiple levels [64]. Secondly, our sample size is relatively small. In the future, we will try to enlarge the sample size including early stage of diabetic nephropathy.

Conclusion and expert recommendations

Spontaneous activity alternations were detected in many areas of the brain, which may provide useful information for understanding the pathology of DRN. Abnormal ALFF values of these brain regions may indicate the development of early DRN and be helpful to predict and prevent early stage of diabetic microvascular lesion.

Table 3 Brain regions alternation and its potential impact

Brain regions	Experimental result	Brain function	Anticipated results
Cerebellum posterior/anterior lobe	DRNs>HCs	Physical balance, motor coordination, the execution of eye movements, emotional processing	Social and emotional problems
Inferior temporal gyrus	DRNs>HCs	Maintain the stability of the neural network	Depression and anxiety
Medial frontal gyrus	DRNs<HCs	Controls spontaneous eye movements, part of the default model network	Mental disorders, including depression and anxiety
Superior temporal gyrus	DRNs<HCs	Associated with ocular diseases	Reflect intraocular inflammation and visual impairment
Middle/inferior frontal gyrus	DRNs<HCs	Part of the default model network	Depression and anxiety
Precuneus	DRNs<HCs	Part of the default model network, the coordination of movement, visuospatial imagery, and working memory	Depression and anxiety
Inferior parietal lobule	DRNs<HCs	Part of the default model network	Depression and anxiety

HCs, healthy controls; *DRN*, diabetic retinopathy with nephropathy

In patients with diabetic retinopathy, diabetic nephropathy or brain dysfunction, delayed diagnosis often delays the optimal time for medical treatment. According to the existing diagnostic criteria, when patients show symptoms of diabetic nephropathy or vision loss and other obvious symptoms, the patient's microvascular lesions have reached a serious degree and the physician could only implement symptomatic treatment. Medical practitioners should move away from the medical model of "delayed reaction" to a "predictive and preventive" approach [65]. The possibility of early diagnosis should be given in the early stage of the disease and medical intervention should be given in the preclinical stage of complications. At present, rs-fMRI technology has been widely used in the early clinical diagnosis of various encephalopathy and eye diseases, and fMRI provides the possibility for predictive, preventive, and personalized medicine (PPPM) model to be practiced in the diagnosis and intervention of diabetic microvascular disease [66]. It also needs more clinical evidence to prove whether screening in populations with suboptimal health status predisposed to diabetes with complications has the same results. To that, of course, this is a highly multidisciplinary and interdisciplinary collaboration task.

Compliance with ethical standards

Conflict of interest The authors declare that they have no conflict of interest.

Consent for publication Not applicable.

Ethical approval All the patients were informed about the purposes of the study and consequently have signed their "consent of the patient." All investigations conformed to the principles outlined in the Declaration of Helsinki and were performed with permission by the responsible Ethics Committee of the First Affiliated Hospital of Nanchang University.

References

1. Vaziri K, Schwartz SG, Relhan N, Kishor KS, Flynn HW. New therapeutic approaches in diabetic retinopathy. Rev Diabet Stud. 2015;12(1–2):196–210. https://doi.org/10.1900/RDS.2015.12.196.
2. Pascolini D, Mariotti SP. Global estimates of visual impairment: 2010. Br J Ophthalmol. 2012;96(5):614–8. https://doi.org/10.1136/bjophthalmol-2011-300539.
3. Frank RN. Diabetic retinopathy. N Engl J Med. 2004;350(1):48–58 10.1056/NEJMra021678.
4. Takagi H. Molecular mechanisms of retinal neovascularization in diabetic retinopathy. Int Congr. 2003;4(3):299. https://doi.org/10.2169/internalmedicine.42.299.
5. Sagoo MK, Gnudi L. Diabetic nephropathy: is there a role for oxidative stress? Free Radic Biol Med. 2018;116:50–63. https://doi.org/10.1016/j.freeradbiomed.2017.12.040.
6. Patel V, Shastri M, Gaur N, Jinwala P, Kadam AY. A study in prevalence of diabetic nephropathy in recently detected cases of type 2 diabetes mellitus as evidenced by altered creatinine clearance, urinary albumin and serum creatinine, with special emphasis on hypertension, hypercholesterolemia and obesity. Int J Adv Med. 2018;5(2):351–5. https://doi.org/10.18203/2349-3933.ijam20180999.
7. Reutens AT. Epidemiology of diabetic kidney disease. Med Clin North Am. 2013;97(1):1–18. https://doi.org/10.1016/j.mcna.2012.10.001.
8. Hamat I, Abderraman GM, Cisse MM, Youssouf M, Djafar MS, Mbainguinam D, et al. Profile of diabetic nephropathy at the National Reference General Hospital of N'Djamena (Chad). Pan Afr Med J. 2016;24:193. https://doi.org/10.11604/pamj.2016.24.193.8415.
9. Caramori ML, Fioretto P, Mauer M. The need for early predictors of diabetic nephropathy risk: is albumin excretion rate sufficient? Diabetes. 2000;49(9):1399–408. https://doi.org/10.2337/diabetes.49.9.1399.
10. Saunders WB. KDOQI clinical practice guidelines and clinical practice recommendations for diabetes and chronic kidney disease. Am J Kidney Dis. 2007;49(2):S12–154. https://doi.org/10.1053/j.ajkd.2006.12.005.
11. Saira C, Sumon R, Andre P, Sayon R. Tight glycemic control regulates fibronectin expression and basement membrane thickening in retinal and glomerular capillaries of diabetic rats. Invest Ophthalmol Vis Sci. 2009;50(2):943–9. https://doi.org/10.1167/iovs.08-2377.

12. Kramer CK, Retnakaran R. Concordance of retinopathy and nephropathy over time in type 1 diabetes: an analysis of data from the diabetes control and complications trial. Diabet Med. 2013;30(11):1333–41. https://doi.org/10.1111/dme.12296.
13. Barrett EJ, Liu Z, Khamaisi M, King GL, Klein R, Klein BEK, et al. Diabetic microvascular disease: an endocrine society scientific statement. J Clin Endocrinol Metab. 2017;102(12):4343–410. https://doi.org/10.1210/jc.2017-01922.
14. Pearce I, Simó R, Lövestam-Adrian M, Wong DT, Evans M. Association between diabetic eye disease and other complications of diabetes: implications for care. A systematic review. Diabetes Obes Metab. 2019;21(3):467–78. https://doi.org/10.1111/dom.13550.
15. Jeng CJ, Hsieh YT, Yang CM, Yang CH, Lin CL, Wang IJ. Diabetic retinopathy in patients with diabetic nephropathy: development and progression. PLoS One. 2016;11(8):e0161897. https://doi.org/10.1371/journal.pone.0161897.
16. Bekiesińska-Figatowska M, Helwich E, Rutkowska M, Stankiewicz J, Terczyńska I. Magnetic resonance imaging of neonates in the magnetic resonance compatible incubator. Arch Med Sci. 2016;12(5):1064–70. https://doi.org/10.5114/aoms.2016.61913.
17. Liu H, Wang X. Correlation of iron deposition and change of gliocyte metabolism in the basal ganglia region evaluated using magnetic resonance imaging techniques: an in vivo study. Arch Med Sci. 2016;12(1):163–71. https://doi.org/10.5114/aoms.2016.57593.
18. Dai XJ, Liu CL, Zhou RL, Gong HH, Wu B, Gao L, et al. Long-term sleep deprivation decreases the default spontaneous activity and connectivity pattern in healthy male subjects: a resting-state fMRI study. Neuropsychiatr Dis Treat. 2015;11:761–72. https://doi.org/10.2147/NDT.S78335.
19. Fox MD, Greicius M. Clinical applications of resting state functional connectivity. Front Syst Neurosci. 2010;4(19):19. https://doi.org/10.3389/fnsys.2010.00019.
20. Zhang Y, Zhu C, Chen H, Duan X, Lu F, Li M, et al. Frequency-dependent alterations in the amplitude of low-frequency fluctuations in social anxiety disorder. J Affect Disord. 2015;174:329–35. https://doi.org/10.1016/j.jad.2014.12.001.
21. Zuo XN, Di Martino A, Kelly C, Shehzad ZE, Gee DG, Klein DF, et al. The oscillating brain: complex and reliable. Neuroimage. 2010;49(2):1432–45. https://doi.org/10.1016/j.neuroimage.2009.09.037.
22. Huang X, Cai FQ, Hu PH, Zhong YL, Zhang Y, Wei R, et al. Disturbed spontaneous brain- activity pattern in patients with optic neuritis using amplitude of low-frequency fluctuation: a functional magnetic resonance imaging study. Neuropsychiatr Dis Treat. 2015;11:3075–83. https://doi.org/10.2147/NDT.S92497.
23. Huang X, Zhong YL, Zeng XJ, Zhong YL, Zhang Y, Wei R, et al. Disturbed spontaneous brain activity pattern in patients with primary angle-closure glaucoma using amplitude of low-frequency fluctuation: a fMRI study. Neuropsychiatr Dis Treat. 2015;11:1877–83. https://doi.org/10.2147/NDT.S87596.
24. Tan G, Huang X, Zhang Y, Wu AH, Zhong YL, Wu K, et al. A functional MRI study of altered spontaneous brain activity pattern in patients with congenital comitant strabismus using amplitude of low-frequency fluctuation. Neuropsychiatr Dis Treat. 2016;12:1243–50. https://doi.org/10.2147/NDT.S104756.
25. Liang M, Xie B, Yang H, Yu L, Yin X, Wei L, et al. Distinct patterns of spontaneous brain activity between children and adults with anisometropic amblyopia: a resting-state fMRI study. Graefes Arch Clin Exp Ophthalmol. 2016;254(3):569–76. https://doi.org/10.1007/s00417-015-3117-9.
26. Alzner E. Bericht vom XXIX. International Congress of Ophthalmology — The World Meeting of Ophthalmologists, 21.–25. April 2002, Sydney — Australien. Spektrum Der Augenheilkunde. 2002;16(4):189–90. https://doi.org/10.1007/BF03164300.
27. Satterthwaite TD, Elliott MA, Gerraty RT, et al. An improved frame- work for confound regression and filtering for control of motion artifact in the preprocessing of resting-state functional connectivity data. Neuroimage. 2013;64:240–56. https://doi.org/10.1016/j.neuroimage.2012.08.052.
28. Yan CG, Cheung B, Kelly C, Gerraty RT, Ruparel K, Loughead J, et al. A comprehensive assessment of regional variation in the impact of head micromovements on functional connectomics. Neuroimage. 2013;76:183–201. https://doi.org/10.1016/j.neuroimage.2013.03.004.
29. Fox MD, Snyder AZ, Vincent JL, Corbetta M, Van Essen DC, Raichle ME. The human brain is intrinsically organized into dynamic, anticorrelated functional networks. Proc Natl Acad Sci U S A. 2005;102(27):9673–8. https://doi.org/10.1073/pnas.0504136102.
30. Li HJ, Dai XJ, Gong HH, Nie X, Zhang W, Peng DC. Aberrant spontaneous low-frequency brain activity in male patients with severe obstructive sleep apnea revealed by resting-state functional MRI. Neuropsychiatr Dis Treat. 2015;11:207–14. https://doi.org/10.2147/NDT.S73730.
31. Dai XJ, Peng DC, Gong HH, Wan AL, Nie X, Li HJ, et al. Altered intrinsic regional brain spontaneous activity and subjective sleep quality in patients with chronic primary insomnia: a resting-state fMRI study. Neuropsychiatr Dis Treat. 2014;10:2163–75. https://doi.org/10.2147/NDT.S69681.
32. Saad ZS, Gotts SJ, Murphy K, Chen G, Jo HJ, Martin A, et al. Trouble at rest: how correlation patterns and group differences become distorted after global signal regression. Brain Connect. 2012;2(1):25–32. https://doi.org/10.1089/brain.2012.0080.
33. Zang YF, He Y, Zhu CZ, Cao QJ, Sui MQ, Liang M, et al. Altered baseline brain activity in children with ADHD revealed by resting-state functional MRI. Brain Dev. 2007;29(2):83–91. https://doi.org/10.1016/j.braindev.2006.07.002.
34. Tomino Y, Gohda T. The prevalence and management of diabetic nephropathy in Asia. Kidney Dis. 2015;1(1):52–60. https://doi.org/10.1159/000381757.
35. Shanbhogue VV, Hansen S, Frost M, Brixen K, Hermann AP. Bone disease in diabetes: another manifestation of microvascular disease? Lancet Diabetes Endocrinol. 2017;5(10):827–38. https://doi.org/10.1016/S2213-8587(17)30134-1.
36. Thapa R, Twyana SN, Paudyal G, Khanal S, van Nispen R, Tan S, et al. Prevalence and risk factors of diabetic retinopathy among an elderly population with diabetes in Nepal: the Bhaktapur Retina Study. Clin Ophthalmol. 2018;12:561–8. https://doi.org/10.2147/OPTH.S157560.
37. Zhao H, Ma L, Yan M, Wang Y, Zhao TT, Zhang HJ, et al. Association between MYH9 and APOL1 gene polymorphisms and the risk of diabetic kidney disease in patients with type 2 diabetes in a Chinese Han population. J Diabetes Res. 2018;1:1–6. https://doi.org/10.1155/2018/5068578.
38. Demerdash FE, Refaie W, Allakany R, Tantawy S, Dawood E. Diabetic retinopathy: a predictor of coronary artery disease. Egyptian Heart J. 2012;64(2):63–8. https://doi.org/10.1016/j.ehj.2011.08.006.
39. Bloomgarden ZT. Diabetic retinopathy and neuropathy. Diabetes Care. 2007;30(3):760. https://doi.org/10.2337/dc07-zb03.
40. Guo MX, Dong HH, Zhang YT, Zhang Q, Yin XH. ALFF changes in brain areas of human with high myopia revealed by resting-state functional MRI. Biomed Eng Inf. 2010;1(1):91–4. https://doi.org/10.1109/BMEI.2010.5639490.
41. Tan G, Huang X, Ye L, Wu AH, He LX, Zhong YL, et al. Altered spontaneous brain activity patterns in patients with unilateral acute open globe injury using amplitude of low-frequency fluctuation: a

functional magnetic resonance imaging study. Neuropsychiatr Dis Treat. 2016;12(1):2015–20. https://doi.org/10.2147/NDT.S110539.
42. Pan ZM, Li HJ, Bao J, Jiang N, Yuan Q, Freeberg S, et al. Altered intrinsic brain activities in patients with acute eye pain using amplitude of low-frequency fluctuation: a resting-state fMRI study. Neuropsychiatr Dis Treat. 2018;14:251–7. https://doi.org/10.2147/NDT.S150051.
43. Li Q, Xin H, Lei Y, Wei R, Zhang Y, Zhong YL, et al. Altered spontaneous brain activity pattern in patients with late monocular blindness in middle-age using amplitude of low-frequency fluctuation: a resting-state functional MRI study. Clin Interv Aging. 2016;11:1773–80. https://doi.org/10.2147/CIA.S117292.
44. Talati A, Hirsch J. Functional specialization within the medial frontal gyrus for perceptual go/no-go decisions based on "what," "when," and "where" related information: an fMRI study. J Cogn Neurosci. 2005;17:981–93. https://doi.org/10.1162/0898929054475226.
45. Bruce CJ, Goldberg ME, Bushnell MC, Stanton GB. Primate frontal eye fields. II. Physiological and anatomical correlates of electrically evoked eye movements. J Neurophysiol. 1985;54:714–34. https://doi.org/10.1152/jn.1985.54.3.714.
46. Zald DH, McHugo M, Ray KL, Glahn DC, Eickhoff SB, Laird AR. Meta-analytic connectivity modeling reveals differential functional connectivity of the medial and lateral orbitofrontal cortex. Cereb Cortex. 2014;24(1):232–48. https://doi.org/10.1093/cercor/bhs308.
47. Lemogne C, Delaveau P, Freton M, Guionnet S, Fossati P. Medial prefrontal cortex and the self in major depression. J Affect Disord. 2012;136(1–2):e1–e11. https://doi.org/10.1016/j.jad.2010.11.034.
48. Garcia A, Luedke A, Dowds E, Tam A, Goel A, Fernandez J. Precuneus volumes and cognitive tests in older adults. Alzheimers Dement. 2013;9(4):P795. https://doi.org/10.1016/j.jalz.2013.05.1638.
49. Liu Y, Li L, Li B, Feng N, Li L, Zhang X, et al. Decreased triple network connectivity in patients with recent onset post-traumatic stress disorder after a single prolonged trauma exposure. Sci Rep. 2017;7(1):12625. https://doi.org/10.1038/s41598-017-12964-6.
50. Vicentini JE, Weiler M, Almeida SRM, de Campos BM, Valler L, Li LM. Depression and anxiety symptoms are associated to disruption of default mode network in subacute ischemic stroke. Brain Imaging Behav. 2017;11(6):1571–80. https://doi.org/10.1007/s11682-016-9605-7.
51. Sieu N, Katon W, Lin EH, Russo J, Ludman E, Ciechanowski P. Depression and incident diabetic retinopathy: a prospective cohort study. Gen Hosp Psychiatry. 2011;33(5):429–35. https://doi.org/10.1016/j.genhosppsych.2011.05.021.
52. Themeli Y, Aliko I, Hashorva A, Bajrami V, Idrizi A, Barbullushi M, et al. P-533 - the correlation between depression and diabetic nephropathy in type 2 diabetes mellitus. Eur Psychiatry. 2012;27:1–1. https://doi.org/10.1016/S0924-9338(12)74700-4.
53. Wallentin M, Weed E, Østergaard L, Mouridsen K, Roepstorff A. Accessing the mental space-spatial working memory processes for language and vision overlap in precuneus. Hum Brain Mapp. 2008;29(5):524–32. https://doi.org/10.1002/hbm.20413.
54. Cavanna AE, Trimble MR. The precuneus: a review of its functional anatomy and behavioural correlates. Brain. 2006;129(3):564–83. https://doi.org/10.1093/brain/awl004.
55. Zhang J, Su J, Wang M, Zhao Y, Yao Q, Zhang Q, et al. Increased default mode network connectivity and increased regional homogeneity in migraineurs without aura. J Headache Pain. 2016;17(1):98. https://doi.org/10.1186/s10194-016-0692-z.
56. Letzen JE, Robinson ME. Negative mood influences default mode network functional connectivity in patients with chronic low back pain: implications for functional neuroimaging biomarkers. Pain. 2017;158(1):48–57. https://doi.org/10.1097/j.pain.0000000000000708.
57. Werring DJ, Bullmore ET, Toosy AT, Miller DH, Barker GJ, MacManus DG, et al. Recovery from optic neuritis is associated with a change in the distribution of cerebral response to visual stimulation: a functional magnetic resonance imaging study. J Neurol Neurosurg Psychiatry. 2000;68(4):441–9. https://doi.org/10.1136/jnnp.68.4.441.
58. Wang ZL, Zou L, Lu ZW, Xie XQ, Jia ZZ, Pan CJ, et al. Abnormal spontaneous brain activity in type 2 diabetic retinopathy revealed by amplitude of low-frequency fluctuations: a resting-state fMRI study. Clin Radiol. 2017;72(4):340.e1–7. https://doi.org/10.1016/j.crad.2016.11.012.
59. Chyzhyk D, Graña M, Öngür D, Shinn AK. Discrimination of schizophrenia auditory hallucinators by machine learning of resting-state functional MRI. Int J Neural Syst. 2015;25(3):1550007. https://doi.org/10.1142/S0129065715500070.
60. Herzfeld DJ, Kojima Y, Soetedjo R, Shadmehr R. Encoding of action by the Purkinje cells of the cerebellum. Nature. 2015;526(7573):439–42. https://doi.org/10.1038/nature15693.
61. Timmann D, Drepper J, Frings M, Maschke M, Richter S, Gerwig M, et al. The human cerebellum contributes to motor, emotional and cognitive associative learning. A review. Cortex. 2010;46(7):845–57. https://doi.org/10.1016/j.cortex.2009.06.009.
62. Morenorius J. The cerebellum in fear and anxiety-related disorders. Prog Neuro-Psychopharmacol Biol Psychiatry. 2018;85:23–32. https://doi.org/10.1016/j.pnpbp.2018.04.002.
63. Ikeda K, Tsuchimochi H, Takeno Y, Yasuda M, Fukushima T, Toyoda K. Clinical analysis of the patients with hemodialysis associated with intracerebral hematoma. No Shinkei Geka. 2004;32(11):1133–7. https://doi.org/10.2176/nmc.44.611.
64. Krapfenbauer K. Identification of beta cell dysfunction at the pre-symptomatic stage of diabetes mellitus by novel analytical system: liquid biopsy measurements in femtograms. EPMA J. 2017;8(1):35–41. https://doi.org/10.1007/s13167-017-0079-5.
65. Duarte AA, Mohsin S, Golubnitschaja O. Diabetes care in figures: current pitfalls and future scenario. EPMA J. 2018;9(2 PG-125-131):125–31. https://doi.org/10.1007/s13167-018-0133-y.
66. Golubnitschaja O, Baban B, Boniolo G, Wang W, Bubnov R, Kapalla M, et al. Medicine in the early twenty-first century: paradigm and anticipation - EPMA position paper 2016. EPMA J. 2016;7(1):1–13. https://doi.org/10.1186/s13167-016-0072-4.